

# Quantifying the uncertainty of neural networks using Monte Carlo dropout for deep learning based quantitative MRI

Mehmet Yigit Avci<sup>1,3</sup>, Ziyu Li<sup>2</sup>, Qiuyun Fan<sup>3,4,5</sup>, Susie Huang<sup>3,4</sup>, Berkin Bilgic<sup>3,4</sup>, Qiyuan Tian<sup>3,4</sup>

<sup>1</sup>*Electrical and Electronics Engineering, Bogazici University, Istanbul, Turkey*, <sup>2</sup>*Nuffield Department of Clinical Neurosciences, University of Oxford, Oxford, UK*, <sup>3</sup>*Martinos Center for Biomedical Imaging, Department of Radiology, Massachusetts General Hospital, Charlestown, MA, USA*, <sup>4</sup>*Harvard Medical School, Boston, USA*, <sup>5</sup>*Department of Biomedical Engineering, College of Precision Instruments and Optoelectronics Engineering, Tianjin University, Tianjin, China*

## Synopsis

*Dropout is conventionally used during the training phase as regularization method and for quantifying uncertainty in deep learning. We propose to use dropout during training as well as inference steps, and average multiple predictions to improve the accuracy, while reducing and quantifying the uncertainty. The results are evaluated for fractional anisotropy (FA) and mean diffusivity (MD) maps which are obtained from only 3 direction scans. With our method, accuracy can be improved significantly compared to network outputs without dropout, especially when the training dataset is small. Moreover, confidence maps are generated which may aid in diagnosis of unseen pathology or artifacts.*

## Introduction

Quantitative MRI is a useful and widely adopted tool to measure tissue properties. However, quantitative MRI often requires specialized sequences and many data samples from a lengthy scan for accurate and robust model fitting, which reduces its feasibility in practice. Emerging deep learning (DL) technologies using neural networks (NNs) have been employed to address this challenge, which have successfully generated high-quality quantitative metrics (e.g., T1, T2, mean diffusivity (MD), fractional anisotropy (FA)) using conventional contrast-weighted images and/or substantially reduced data.

Nonetheless, the uncertainty of these DL methods has rarely been characterized, which is as important as their accuracy. NNs may fail to generalize to test images that are not well represented by the training data (e.g., due to the use of different hardware and imaging protocols and the presence of artifacts and structural pathology). It is therefore crucial to quantify the uncertainty/confidence of NNs for risk management and potential human intervention on failure cases.

Monte Carlo dropout (MCDropout) provides an effective and practical approach to quantify the uncertainty of NNs, without changing their architectures or the optimisation. Dropout, which randomly switches off neurons in a NN during training (inactive during inference), is a useful regularizer to avoid overfitting. It was recently shown that using dropout also during inference can be interpreted as a Bayesian approximation of the Gaussian process [cite]. Each dropout configuration, corresponding to a sub-network with slightly varying architecture, yields a different prediction as a sample from the approximate parametric posterior

distribution (Fig.1a). The uncertainty can be then quantified as the variance of numerous predictions (e.g., 30~100). Additionally, averaging predictions from many dropout configurations also achieves improved accuracy (i.e., model averaging).

We propose to employ MCDropout for quantifying the uncertainty and improving the performance of NNs and preventing overfitting for DL-based quantitative MRI. We demonstrate its effectiveness on a challenging task for synthesizing high-quality FA and MD values from one  $b=0$  image and three diffusion-weighted image (DWI) volumes. (Code/data: [https://anonymous.4open.science/r/dropout\\_ISMRM-4102/](https://anonymous.4open.science/r/dropout_ISMRM-4102/))

## Methods

**Data.** Pre-processed diffusion MRI data (1.25mm isotropic,  $18 \times b=0$ ,  $90 \times b=1000$  s/mm<sup>2</sup>) of 42 subjects (10 for testing) from the Human Connectome Project (HCP), WU-Minn-Ox Consortium were used. For each subject, the first  $b=0$  image and three DWI volumes along orthogonal directions were extracted. Tensor fitting was performed on all volumes using FSL's "dtifit" function to generate ground-truth FA and MD volumes. The brain segmentation from FreeSurfer reconstruction of T1-weighted data ("aseg") was resampled to the diffusion image space to generate binarized masks of brain structures.

**Training.** A 3D U-Net (5 depths, 32 kernels at first depth) was modified to include dropout layers for decoding (Fig.1b, entitled "DU-Net"), which was essentially an U-Net if dropout rates were set to 0. NNs were implemented using the Keras API (<https://keras.io/>) with a Tensorflow (<https://www.tensorflow.org/>) backend. Training was performed on  $64 \times 64 \times 64$  blocks (80% for training, 20% for validation) with Adam optimizers using Google Colaboratory. L1 loss was only computed within the brain parenchyma.

**Evaluation.** Experiments were performed with different numbers of training subjects (1~32) and dropout rates (0~0.7). The uncertainty was calculated as the standard deviation over mean of 100 predictions for each voxel. The final synthesized results were calculated as the average of 1~100 predictions. The mean absolute errors (MAEs) between NN-synthesized and ground-truth FA and MD values were calculated within the brain parenchyma and averaged for measuring accuracy.

## Results

Exemplar FA predictions from two dropout configurations were slightly different as expected (Fig.2a-c) whereas the difference is low between two averaged results (Fig.2d-f). The uncertainty map for FA was spatially varying (Fig.2g,h) and tissue-dependent (Fig.2j). Quantitatively, the uncertainty was lower in the white matter (0.0478) than in the cerebral (0.0756) and deep gray matter and was lowest in the corpus callosum (0.0288).

Figure 3 demonstrates the capability of uncertainty quantification for detecting artifacts unseen in the training data (i.e., voxels within the letter "M" set to very bright or dark). Uncertainty maps clearly exhibited increased uncertainty within the letter "M". The FA synthesis was more sensitive to the voxel intensity increase, while MD synthesis was more sensitive to voxel intensity decrease.

Dropout also increased the synthesis accuracy (Fig.4). Even a single prediction from DU-Net outperformed that from a standard U-Net dropout for FA and MD (with 1~4 training subjects). The average of 100 predictions from DU-Net achieved even higher accuracy. The improvement was most significant when the number of subjects for training was limited (1~4 subjects, 15%~25% lower MAE) since dropout avoided overfitting. Averaging predictions from DU-Net training on data from one subject had almost equivalent performance compared to results from U-Net trained on data from four subjects.

Figure 5 demonstrated that 0.2 was the optimal dropout rate for achieving the highest accuracy, and averaging more predictions led to higher accuracy while performance plateaued after averaging 50 predictions.

## Discussion and Conclusion

MCDropout provides a useful tool for quantifying the uncertainty and improving the predictive accuracy of NNs for safer and better synthesis of quantitative metrics, which does not add training overhead or change the architecture of NNs and only adds minimal cost to inference time. MCDropout can be easily used for any other networks (variational/unrolled network) and tasks (reconstruction, denosing, superresolution, segmentation, classification) for MRI.

## Acknowledgments

The T1w data at 0.7 mm isotropic resolution and diffusion data at 1.25 mm isotropic resolution were provided by the Human Connectome Project, WU-Minn-Ox Consortium (Principal Investigators: David Van Essen and Kamil Ugurbil; U54-MH091657) funded by the 16 NIH Institutes and Centers that support the NIH Blueprint for Neuroscience Research; and by the McDonnell Center for Systems Neuroscience at Washington University. This work was supported by the National Institutes of Health (grant numbers P41-EB015896, P41-EB030006, U01-EB026996, U01-EB025162, S10-RR023401, S10-RR019307, S10-RR023043, R01-EB028797, R03-EB031175, K99-AG073506), the NVidia Corporation for computing support, and the Athinoula A. Martinos Center for Biomedical Imaging.

## References

1. Golkov V, Dosovitskiy A, Sperl JI, et al. q-Space deep learning: twelve-fold shorter and model-free diffusion MRI scans. *IEEE transactions on medical imaging*. 2016;35(5):1344-1351.
2. Qiu S, Chen Y, Ma S, et al. Multiparametric mapping in the brain from conventional contrast-weighted images using deep learning. *Magnetic Resonance in Medicine*. 2021.
3. Tian Q, Bilgic B, Fan Q, et al. DeepDTI: High-fidelity six-direction diffusion tensor imaging using deep learning. *NeuroImage*. 2020;219:117017.
4. Aliotta E, Nourzadeh H, Patel SH. Extracting diffusion tensor fractional anisotropy and mean diffusivity from 3-direction DWI scans using deep learning. *Magnetic Resonance in Medicine*.
5. Sveinsson B, Chaudhari AS, Zhu B, et al. Synthesizing Quantitative T2 Maps in Right Lateral Knee Femoral Condyles from Multi-Contrast Anatomical Data with a Conditional GAN. *Radiology: Artificial Intelligence*. 2021:e200122.
6. Gal Y, Ghahramani Z. Dropout as a bayesian approximation: Representing model uncertainty in deep learning. Paper presented at: international conference on machine learning2016.
7. Falk T, Mai D, Bensch R, et al. U-Net: deep learning for cell counting, detection, and morphometry. *Nature Methods*. 2019;16(1):67-70.
8. Gong E, Pauly JM, Wintermark M, Zaharchuk G. Deep learning enables reduced gadolinium dose for contrast-enhanced brain MRI. *Journal of Magnetic Resonance Imaging*. 2018;48(2):330-340.
9. Chen KT, Gong E, de Carvalho Macruz FB, et al. Ultra-Low-Dose 18F-Florbetaben Amyloid PET Imaging Using Deep Learning with Multi-Contrast MRI Inputs. *Radiology*. 2018;290(3):649-656.
10. Sotiroopoulos SN, Jbabdi S, Xu J, et al. Advances in diffusion MRI acquisition and processing in the Human Connectome Project. *NeuroImage*. 2013;80:125-143.
11. Glasser MF, Sotiroopoulos SN, Wilson JA, et al. The minimal preprocessing pipelines for the Human Connectome Project. *NeuroImage*. 2013;80:105-124.
12. Glasser MF, Smith SM, Marcus DS, et al. The human connectome project's neuroimaging approach. *Nature Neuroscience*. 2016;19(9):1175-1187.

## Figures

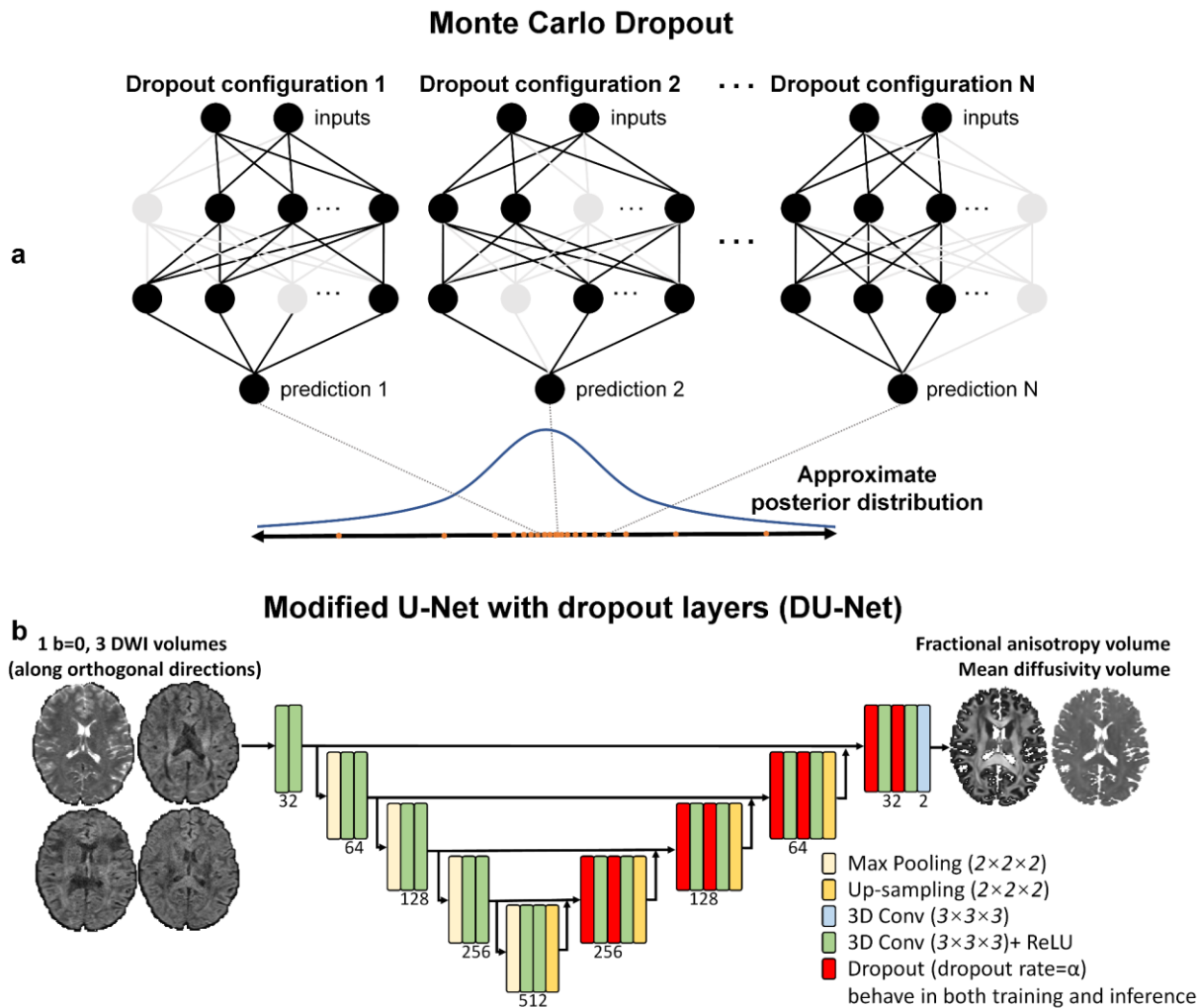


**Figure 1. Monte Carlo dropout.** The modified 3D U-Net includes dropout layers stacked with convolutional layers for decoding (a), which becomes a standard U-Net if the dropout rate is set to 0. Dropout layers behave in both training and inference. The input includes 1  $b=0$  image volume and 3 diffusion-weighted image volumes along orthogonal directions. The output includes two volumes of fractional anisotropy and mean diffusivity values.

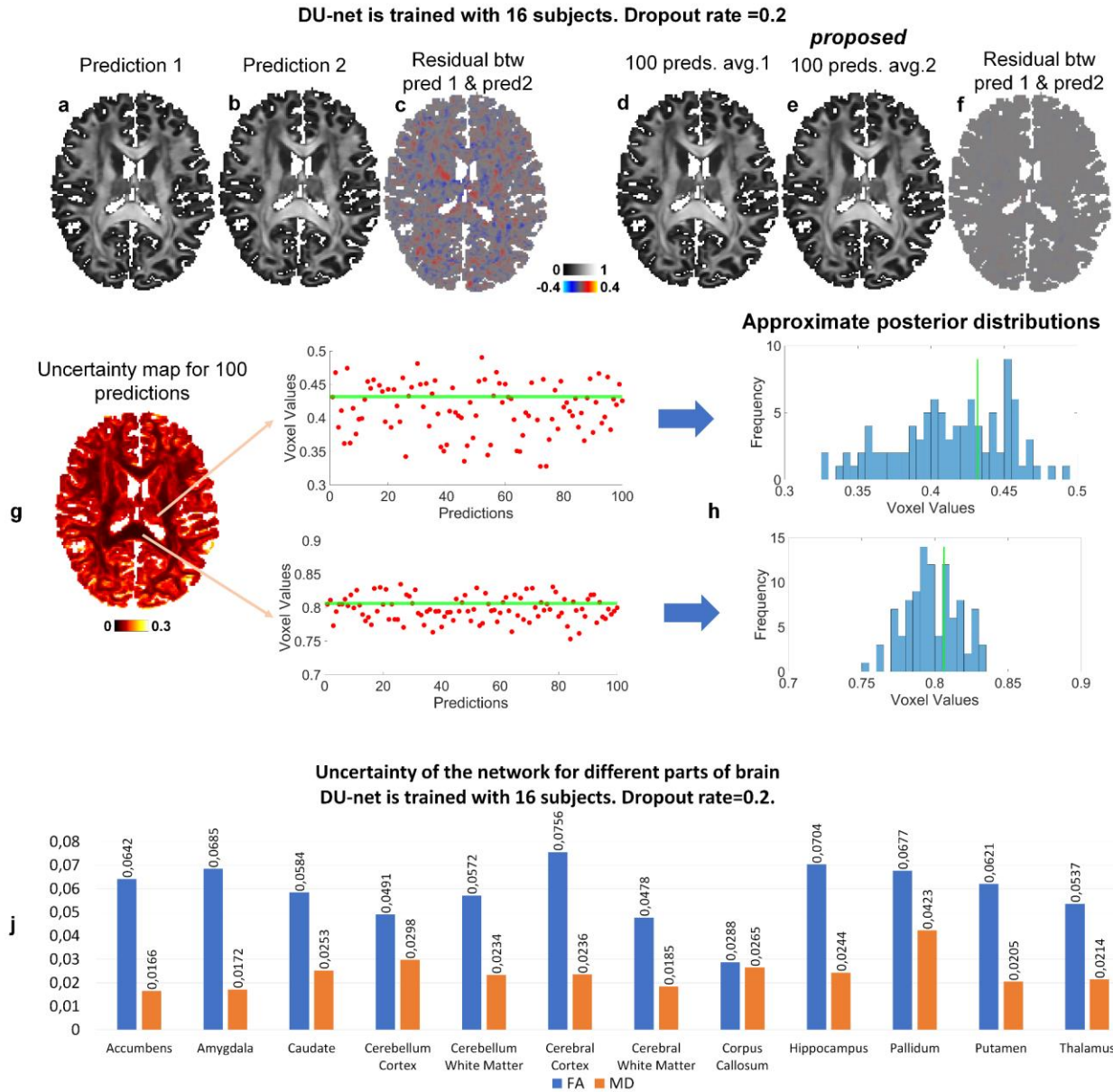


**Figure 2. Effects of averaging on uncertainty.** Difference (d) between two predictions (a,b) and difference (f) between 100 predictions and another 100 predictions averaged (d,e) for FA maps. Uncertainty map (g) for 100 predictions along with 100 predictions and ground truth of a single voxel from white matter with low uncertainty, and gray matter with high uncertainty, also their histogram (h). Uncertainty in different tissue types in the brain (tested for 10 subjects and took their mean) (j) .

Results for a subject with artificial artifacts.  
DU-net is trained with 16 subjects. Dropout rate=0.2.

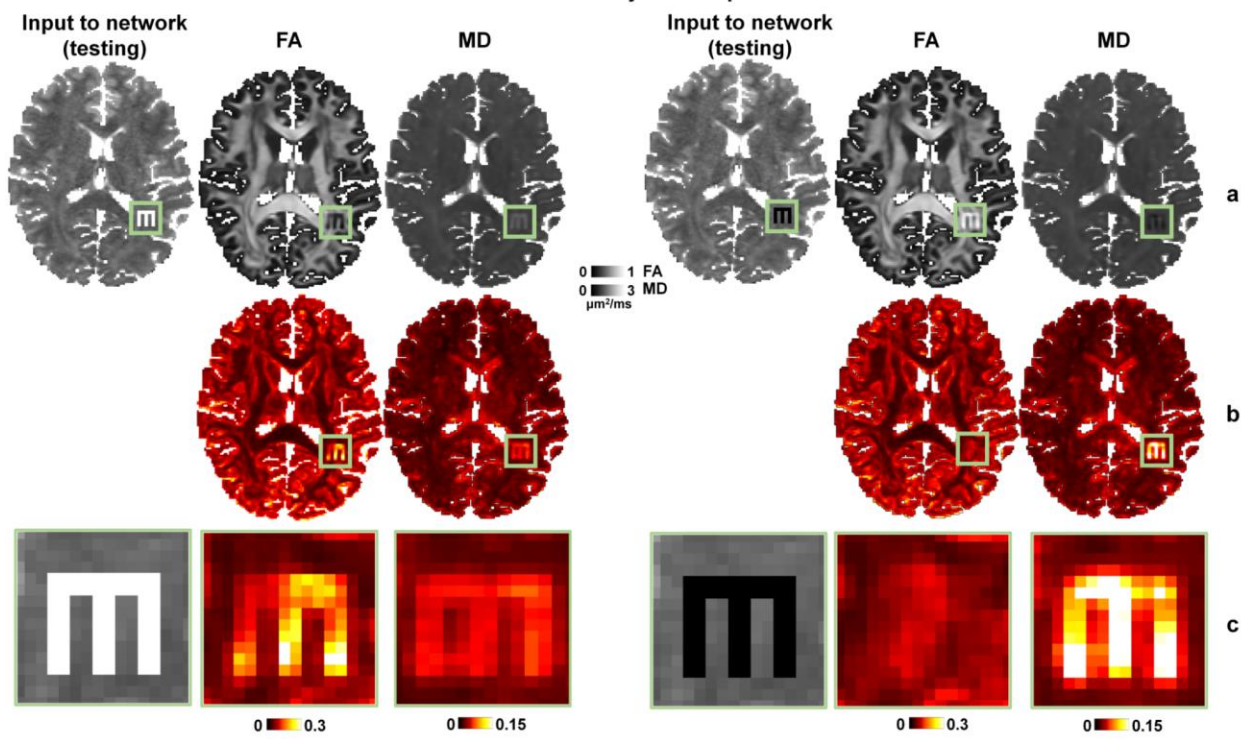


**Figure 3. Results for a subject with artificial artifacts.** Synthesized FA and MD maps obtained by averaging 100 predictions for the subject with artificial artifacts (a). Uncertainty maps (b) for corresponding results in (a), and enlarged regions (c).

DU-net models are trained with 16 subjects. Dropout rate=0.2. Ground truth is generated from 90dwi fitted tensor. DU-net outputs are generated from 3dwi + 1b0. **proposed**

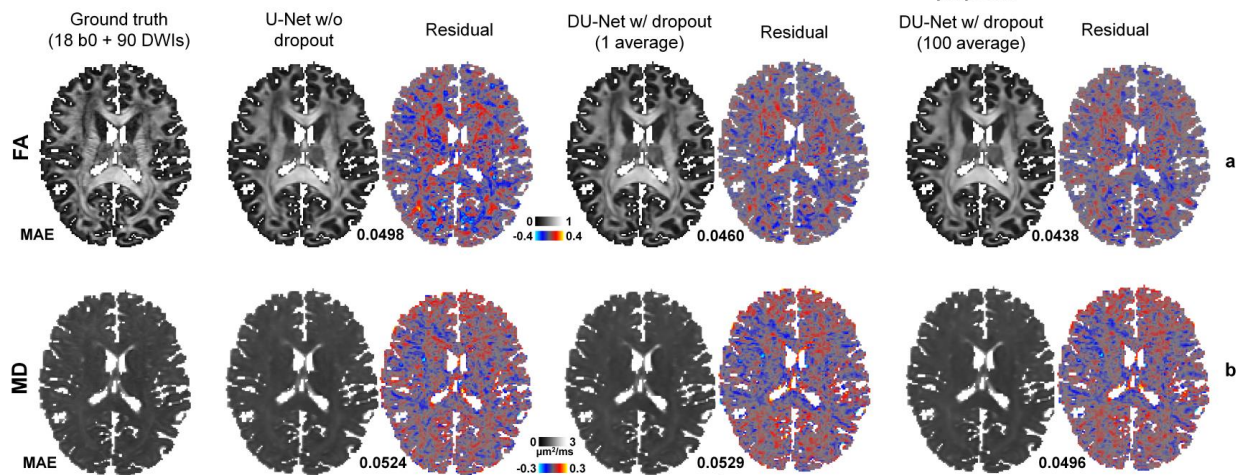


**Figure 4. Comparison of standard and proposed network.** Results of U-net without dropout, 1 prediction and 100 predictions avg. for both FA (a) and MD (b). Mean absolute error (MAE) between results and the ground truth (tested for 10 subjects and took their mean) of different numbers of subjects for training are given in the tables (c), with improvement in MAE between 100 predictions of U-net with dropout averaged, and a prediction of standard U-net.

Number of subj. for training	MAE (MD) ( $\mu\text{m}^2/\text{ms}$ )			
	W/o dropout	1 pred. drop rate=0.2	100 preds. drop rate=0.2	Improvement (%) (100 preds. vs w/o dropout)
32 subjects	0.0490	0.0504	<b>0.0475</b>	3.061
16 subjects	0.0524	0.0529	<b>0.0496</b>	5.343
8 subjects	0.0557	0.0559	<b>0.0523</b>	6.104
4 subjects	0.0650	0.0594	<b>0.0551</b>	15.231
2 subjects	0.0796	0.0662	<b>0.0604</b>	24.121
1 subject	0.0818	0.0670	<b>0.0615</b>	24.817

Number of subj. for training	MAE (FA)			
	W/o dropout	1 pred. drop rate=0.2	100 preds. drop rate=0.2	Improvement (%) (100 preds. vs w/o dropout)
32 subjects	0.0458	0.0434	<b>0.0414</b>	9.606
16 subjects	0.0498	0.0460	<b>0.0438</b>	12.048
8 subjects	0.0525	0.0491	<b>0.0469</b>	10.666
4 subjects	0.0589	0.0536	<b>0.0511</b>	13.243
2 subjects	0.0694	0.0596	<b>0.0568</b>	18.155
1 subject	0.0733	0.0622	<b>0.0595</b>	18.827

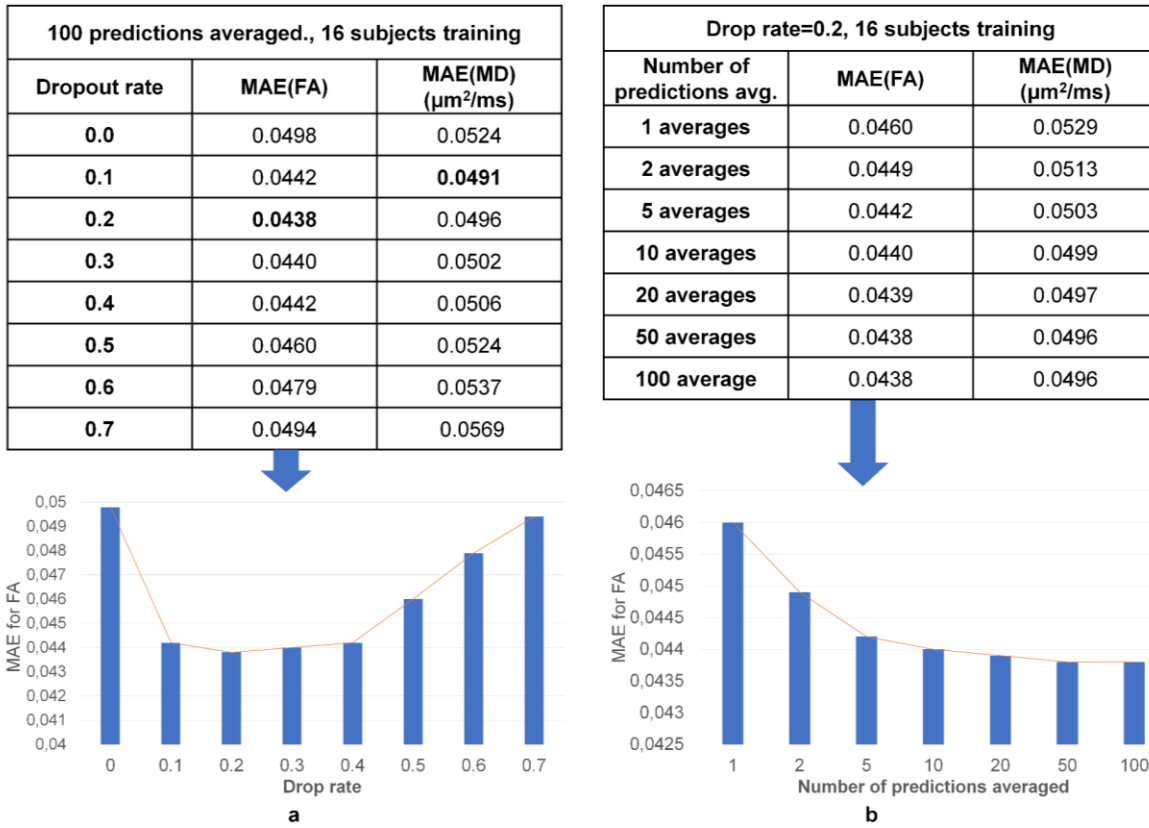


**Figure 5. Results for different experiments.** Results of different cases in terms of MAE (tested for 10 subjects and took their mean) for varying drop rate (a), and varying number of times predictions averaged (b). Increasing drop rate, results in a bell-shaped curve for MAE, with optimum drop rate 0.2 for this case (a). Improvement saturates after a certain number of predictions, while it increases rapidly in the beginning for the lower number of predictions (b).